Development of a Thermo-Hydro-Geochemical Model for Low Temperature Geoexchange Applications

F. Eppner*[1], P. Pasquier[1], and P. Baudron[1]
[1] Department of Civil, Geological and Mining Engineering, Polytechnique Montreal
*Corresponding author: P.O. Box 6079 Station Centre-Ville, Montreal, Canada H3C 3A7, fanny.eppner@polymtl.ca

Abstract: Low temperature geoexchange systems are used to provide space heating and cooling to buildings. Some of these systems use groundwater as heat carrier fluid, which may promote calcite scaling and increase maintenance costs. A fully coupled multiphysics model was implemented allowing simulation of the thermo-hydro-geochemical processes within a standing column well and the geological formation. Three physics are used to link species advection, diffusion and temperature dependent reactions. Dissolution and precipitation of calcite is modeled as reaction kinetics based on empirical model while species' activities are computed at equilibrium by solving locally on the domain algebraic equations. The results demonstrate that calcite dissolution and precipitation may occur in the system during a typical 1-year operation. However, the bleed may have a positive effect on the chemical parameters, thus limiting the risks of precipitation.

Keywords: standing column well, THG model, hydrogeochemistry, calcite, PWP model.

1. Introduction

With the aim of providing space heating and cooling to buildings and reducing their energy consumption, ground-source heat pump systems using standing column wells (SCW) as ground heat exchanger are increasingly studied. In such systems, groundwater is pumped at the base of the well and directed to a heat exchanger (Figure 1) where heat is exchanged with a building through a heat pump. The pumped water can be re-injected at the top of the well or discharged in an injection well to increase circulation of groundwater through the aquifer. This operation, called bleed, helps stabilizing the fluid temperature and enhance the thermal efficiency of the heat pump.

Since SCWs use groundwater directly as heat carrier fluid, the temperature of the fluid is continuously modified depending on the building heating and cooling loads. This will modify the fluid chemical equilibrium, which may promote calcite dissolution and precipitation in the well and surrounding aquifer, heat exchanger and pipes, and eventually affect their efficiency and maintenance costs.

Several SCW models coupling heat transfer and groundwater flow already exist (Abu-Nada and al., 2008; Deng and al., 2005; Ng and al., 2011; Rees and al., 2004; Nguyen and al., 2012, 2015a, 2015b). However, no model allows integration of geochemical reactions and realization of coupled thermo-hydro-geochemical (THG) simulations. The objective of this paper is to present a fully coupled multiphysics model integrating reaction kinetics and ensuring chemical equilibrium to study the THG processes occurring in a SCW and its surrounding aquifer.

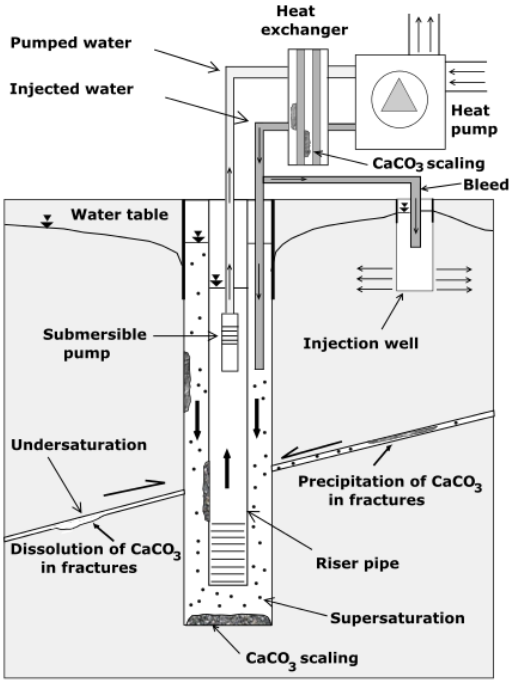

Figure 1. Illustration of a standing column well system and geochemical processes involving calcite.

2. Numerical model

The model presented in this paper is developed within the Comsol Multiphysics environment and uses three different physics from the Subsurface flow module (Darcy's Law, Heat transfer in porous media and Solute transport) as well as the global ODEs and DAEs node to ensure local chemical equilibrium.

The SCW model studied in this work represents a well having a length of 300 m, a radius of 0.102 m and equipped with a riser pipe having inner and outer diameters of 0.070 m and 0.076 m respectively. The SCW is modelled through a 2D axisymmetric geometry with a vertical lateral boundary located 40 m away from the revolution axis.

The groundwater flow and heat transfer models are inspired by the work of Nguyen and al. (2012, 2015a) and additional details can be found in these references. However, for sake of completeness, the main features of these models are described hereinafter, along with the geochemical model added in this work to simulate transport of dissolved chemical species.

2.1 Groundwater flow model

Conservation equation and Darcy's law govern the saturated flow in the domain and are expressed by:

$$\rho S \frac{\partial p}{\partial t} + \nabla \cdot (\rho v) = 0 \qquad (1)$$

$$v = -\frac{K}{\rho g}(\nabla p + \rho g \nabla D_v) \qquad (2)$$

where ρ is the fluid density (kg/m^3), S is the storage coefficient (1/Pa), p is the pressure (Pa), t is the time (s), v is Darcy's velocity (m/s), K is the hydraulic conductivity (m/s), g is the gravitational acceleration (m/s^2) and D_v is the vertical coordinate (m).

The fluid velocity (m/s) in the subdomains corresponding respectively to the ascending and descending fluid (v_o *and* v_i) are specified by:

$$v_o = \frac{\dot{V}}{A_o} \quad , \quad v_i = \frac{\dot{V}(1-B)}{A_i} \qquad (3a,b)$$

where $\dot{V}$ is the total pumping rate (m^3/s), A_o is the cross sectional area of the riser pipe (m^2), A_i is the area of the annular space between the borehole wall and the outer pipe surface (m^2) and B is a parameter varying between 0 and 1, which corresponds to the normalized bleed flow rate (-). Thus when $B=0$, all the pumped water is re-injected inside the well whereas when $B=1$, the pumped water is completely discharged outside the well.

The geometry and boundary conditions of the flow model are summarized in Figure 2. A no flux boundary is defined at the top and at the base of the aquifer while a constant hydraulic head of 310 m is imposed along the lateral boundary. A homogeneous hydraulic head of 310 m is used as the initial solution of the problem. Table 1 presents the hydrogeological parameters used to solve the problem.

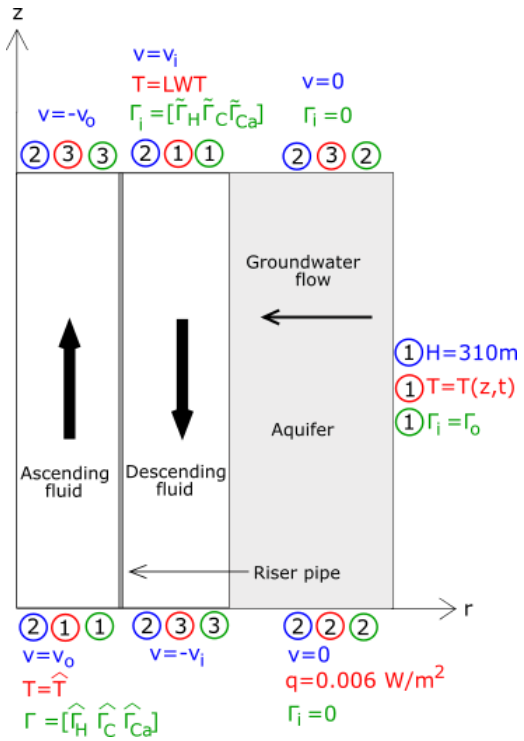

Figure 2. Simplified representation of a SCW and boundary conditions for the fluid flow model (blue), the heat transfer model (red) and the geochemical model (green). Legend: 1 for Dirichlet, 2 for Neumann, 3 for open boundary, *LWT* for leaving water temperature, q for heat flux, ˜ for the mean value evaluated at the riser pipe outflow and ^ for the mean value evaluated at the base of the annular space.

Table 1: Hydraulic and heat transfer parameters.

Para.	Fluid	Soil	Pipe	Units
ρ	1e3	2.7e3	1.3e3	kg/m^3
φ	1.0	0.1	1e-5	-
K	1e3	2e-6	1e-9	m/s
μ	1e-3	-	-	m^2
D_f	1e-2	1e-9	-	m^2/s
D_p	1	0	-	m
k	0.6	2.5	9.74e-2	W/(K·m)
C_p	4.2e3	8e2	1.2e3	J/(K·kg)

2.2 Heat transfer model

The governing equation solved for the heat transfer model is:

$$\rho C_p \frac{\partial T}{\partial t} + \rho C_p v \cdot \nabla T = \nabla \cdot (\lambda \nabla T) \qquad (4)$$

where λ and ρC_p are the equivalent thermal conductivity (W/(K·m)) and volumetric heat capacity (J/(K·m^3)) and where T is the groundwater temperature (K).

The heat pump and heat exchanger are not simulated directly but integrated through:

$$LWT = EWT + \frac{\dot{Q}_g}{\dot{V} \cdot \rho \cdot cp} \qquad (5)$$

where EWT and LWT are the heat pump' entering and leaving water temperature respectively and $\dot{Q}_g$ corresponds to the load extracted or transmitted from/to the ground (W). EWT is obtained by a boundary integration over the area of the riser pipe at the top of the model. In fact, the last term in Eq. 5 corresponds to the temperature variation induced by the heat pump operation for a perfectly efficient heat exchanger.

The initial temperature of the system and the temperature along the vertical lateral boundary are defined by the Lunardini (1981) equation which integrates the ground seasonal temperature variations and depth. Moreover, at the base of the aquifer, a geothermal heat flux of 0.006 W/m^2 is imposed. The top and base of the aquifer are defined as open boundaries. The temperature imposed along the base of the ascending fluid subdomain corresponds to the mean temperature evaluated along the base of the annular space. Table 1 presents the parameters of the heat transfer model while the boundary conditions of the heat transfer model are illustrated in Figure 2.

2.3 Geochemical model

Saaltink and al. (1998) presented a mathematical formulation allowing simulating efficiently transport of dissolved chemical species when kinetics and equilibrium reactions interfere with the species' activities. Following the notation of Holzbecher (2012), the governing equation solved to link advection-diffusion of species with kinetics and equilibrium reactions is:

$$\varphi \frac{\partial}{\partial t} \boldsymbol{\Gamma} = \nabla \cdot (D \nabla \boldsymbol{\Gamma}) - \nabla \cdot (v \boldsymbol{\Gamma}) + \boldsymbol{U S_k' r_k} \qquad (6)$$

where φ is the ground porosity (-), $\boldsymbol{\Gamma}$ is the vector of species' total activity (kg/m^3), D is the diffusion coefficient of the total activity (m^2/s) which includes the molecular diffusion D_f and dispersivity D_p. In Eq. 6, $\boldsymbol{U}$ is a transformation matrix, $\boldsymbol{S_k}$ is the stoichiometric matrix for reaction kinetics, $\boldsymbol{r_k}$ is a column vectors of reaction rates for reaction kinetics (Eq. 8) and $'$ is the transpose operator. These matrix and vectors will be defined in the next subsections. Notice that v in Eq. 6 is the groundwater velocity computed by the groundwater flow model.

In this work, the following nine chemical species are considered: $\boldsymbol{\alpha_i}$= [α_1=H^+ α_2=HCO_3^- α_3=Ca^{2+} α_4=OH^- α_5=H_2CO_3 α_6=CO_3^{2-} α_7=$CaHCO_3^+$ α_8=$CaCO_{3(aq)}$ α_9=$CaOH^+$]'. With the aim to considerably simplify the model, the species are grouped according to the Tableaux method in three total activities $\boldsymbol{\Gamma_j}$ = [Γ_H Γ_C Γ_{Ca}]', thus allowing solving only three advection-diffusion equations (Eq. 6) instead of nine.

The Tableaux method (Morel and Hering, 1993) with H^+, HCO_3^- and Ca^{2+} as basis components is used to define the total activities. The principle is to add or subtract a linear combination of basis components to form the species contained in vector $\boldsymbol{\alpha_i}$. The next step is to create a table with the rows corresponding to the species and the column to the components as shown in Table 2. The table contains the stoichiometric coefficients of each component needed to form each species. In this work, the three total activities defined from Table 2 are:

$$\Gamma_H = \alpha_1 - \alpha_4 + \alpha_5 - \alpha_6 - \alpha_8 - \alpha_9 \qquad (7a)$$

$$\Gamma_C = \alpha_2 + \alpha_5 + \alpha_6 + \alpha_7 + \alpha_8 \qquad (7b)$$

$$\Gamma_{Ca} = \alpha_3 + \alpha_7 + \alpha_8 + \alpha_9 \qquad (7c)$$

Table 2: Illustration of the Tableaux method.

α	Species	Components		
		H	*C*	*Ca*
α_1	$(H^+)_1$	1	0	0
α_2	$(HCO_3^-)_1$	0	1	0
α_3	$(Ca^{2+})_1$	0	0	1
α_4	$(H_2O)_1(H^+)_{-1}$	-1	0	0
α_5	$(HCO_3^-)_1(H^+)_1$	1	1	0
α_6	$(HCO_3^-)_1(H^+)_{-1}$	-1	1	0
α_7	$(Ca^{2+})_1(HCO_3^-)_1$	0	1	1
α_8	$(H^+)_{-1}(HCO_3^+)_1(Ca^{2+})_1$	-1	1	1
α_9	$(H_2O)_1\,(H^+)_{-1}(Ca^{2+})_1$	-1	0	1

2.4.1 Reaction Kinetics

Plummer and al., (1978) proposed the Plummer, Wigley and Parkhurst (PWP) model allowing to express precipitation and dissolution of calcite through the three following elementary reactions:

$$CaCO_3 + H^+ \underset{k_{-1}}{\overset{k_1}{\rightleftharpoons}} Ca^{2+} + HCO_3^- \quad (8a)$$

$$CaCO_3 + H_2CO_3° \underset{k_{-2}}{\overset{k_2}{\rightleftharpoons}} Ca^{2+} + 2HCO_3^- \quad (8b)$$

$$CaCO_3 + H_2O \underset{k_{-3}}{\overset{k_3}{\rightleftharpoons}} Ca^{2+} + HCO_3^- + OH^- \quad (8c)$$

where k_1, k_2 and k_3 denote the rate constant for the direct reactions (m/s) and k_{-1} ($m^4/kg{\cdot}s$), k_{-2} ($m^7/kg^2{\cdot}s$) and k_{-3} ($m^7/kg^2{\cdot}s$) are the rate constants for the reverse reactions. Notice that in Eq. 8b, $CO_{2(aq)}$ + $H_2CO_3°$ corresponds to H_2CO_3*. Even if $H_2CO_3°$ and $CO_{2(aq)}$ are different species, they are often considered as a single species and the sum of the activities corresponds to the activity of H_2CO_3*.

The rate constants controlling the speed of the reactions are temperature dependent and are calculated as follow:

$$k_1 = 10^{\left(0.198\frac{444}{T}\right)} \quad k_2 = 10^{\left(2.84-\frac{2177}{T}\right)} \quad (9a,b)$$

$$k_3 = 10^{\left(-5.86-\frac{317}{T}\right)} \; for\; T < 25^\circ C \quad (9c)$$

$$k_3 = 10^{\left(-1.10-\frac{1737}{T}\right)} \; for\; T > 25°C \quad (9d)$$

where T is the temperature of the groundwater (K). Knowing the equilibrium constants of the reactions ($K_{eq\,j}$) for a given temperature, the rate constants for the reverse reactions (k_{-j}) are obtained by:

$$k_{-j} = \frac{k_j}{K_{eq\,j}} \quad (10)$$

where k_j are the direct reaction rate constants (variable units).

The reaction rate of a reaction (R_j) calculated in function of the species' activities and the rate constants allows computation of the temporal variation of the activities of reactants (r) and products (p) as follow:

$$R_j = k_{+j} \cdot \alpha_{r,j} - k_{-j} \cdot \alpha_{p,j} \quad (11)$$

$$\frac{\partial \alpha_{r,j}}{\partial t} = -R_j \quad , \quad \frac{\partial \alpha_{p,j}}{\partial t} = +R_j \quad (12a,b)$$

Matrix $\boldsymbol{U}$ is defined from Table 2 while vector $\boldsymbol{S'_k r_k}$ is deduced from Eq. 12a and 12b. In matrix notation, $\boldsymbol{U}$ and $\boldsymbol{S'_k r_k}$ are given by:

$$\boldsymbol{U'} = \begin{matrix} \Gamma_H & \Gamma_C & \Gamma_{Ca} \\ \end{matrix} \begin{bmatrix} 1 & 0 & 0 \\ 0 & 1 & 0 \\ 0 & 0 & 1 \\ -1 & 0 & 0 \\ 1 & 1 & 0 \\ -1 & 1 & 0 \\ 0 & 1 & 1 \\ -1 & 1 & 1 \\ -1 & 0 & 1 \end{bmatrix} \begin{matrix} \alpha_1 \\ \alpha_2 \\ \alpha_3 \\ \alpha_4 \\ \alpha_5 \\ \alpha_6 \\ \alpha_7 \\ \alpha_8 \\ \alpha_9 \end{matrix} \quad \boldsymbol{S'_k r_k} = \begin{matrix} \partial\alpha/\partial t \\ \end{matrix} \begin{bmatrix} -R_1 \\ R_1 + 2R_2 + R_3 \\ R_1 + R_2 + R_3 \\ R_3 \\ -R_2 \\ 0 \\ 0 \\ 0 \\ 0 \end{bmatrix} \begin{matrix} \alpha_1 \\ \alpha_2 \\ \alpha_3 \\ \alpha_4 \\ \alpha_5 \\ \alpha_6 \\ \alpha_7 \\ \alpha_8 \\ \alpha_9 \end{matrix}$$

where R_1, R_2 and R_3 are the overall rate of reaction ($kg/(m^2{\cdot}s)$) of Eq. 8a to 8c obtained with Eq. 11. Finally, the temporal variation of the three total activities are integrated in the model through a reaction term as follow:

$$\boldsymbol{U S'_k r_k} = \begin{bmatrix} -R_1 - R_2 - R_3 \\ R_1 + R_2 + R_3 \\ R_1 + R_2 + R_3 \end{bmatrix} \quad (13)$$

Notice that the reaction rates must be multiplied by the ratio of the area of calcite to the volume of solution (A/V) to express them in $kg/(m^3{\cdot}s)$, as required by the Solute transport module.

2.4.2 Equilibrium reactions

In this work, the equilibrium reactions used to simulate the carbonate system are:

$$H^+ + OH^- \rightleftharpoons H_2O \quad (14a)$$

$$H^+ + CO_3^{2-} \rightleftharpoons HCO_3^- \quad (14b)$$

$$Ca^{2+} + HCO_3^- \rightleftharpoons CaHCO_3^+ \quad (14c)$$

$$H^+ + HCO_3^- \rightleftharpoons H_2CO_3 \quad (14d)$$

$$Ca^{2+} + CO_3^{2-} \rightleftharpoons CaCO_{3(aq)} \quad (14e)$$

$$H^+ + CaOH^+ \rightleftharpoons Ca^{2+} + H_2O \quad (14f)$$

The equilibrium constant can be written in a matrix form as follow (Holzbecher, 2012):

$$\boldsymbol{S_e} \cdot \log \boldsymbol{\alpha} = \log \boldsymbol{K} \quad (15)$$

with $n_{ji} = m_i^{(j)} - n_i^{(j)}$ and $\boldsymbol{S_e} = (n_{ji})$. $\boldsymbol{S_e}$ is a reaction matrix with N_s (number of species) columns and N_r (number of equilibrium reactions) rows, $\boldsymbol{\alpha}$ and $\boldsymbol{K}$ are two vectors containing species' activities and equilibrium constants and m and n are stoichiometric coefficients for reactants and products respectively (-). Thus the reaction matrix $\boldsymbol{S_e}$, containing the stoichiometric coefficients, is defined by:

$$\boldsymbol{S_e} = \begin{matrix} \alpha_1 & \alpha_2 & \alpha_3 & \alpha_4 & \alpha_5 & \alpha_6 & \alpha_7 & \alpha_8 & \alpha_9 & \\ \end{matrix} \begin{bmatrix} 1 & 0 & 0 & 1 & 0 & 0 & 0 & 0 & 0 \\ 1 & -1 & 0 & 0 & 0 & 1 & 0 & 0 & 0 \\ 0 & 1 & 1 & 0 & 0 & 0 & -1 & 0 & 0 \\ 1 & 1 & 0 & 0 & -1 & 0 & 0 & 0 & 0 \\ 0 & 0 & 1 & 0 & 0 & 1 & 0 & -1 & 0 \\ 1 & 0 & -1 & 0 & 0 & 0 & 0 & 0 & 1 \end{bmatrix} \begin{matrix} \text{14a} \\ \text{14b} \\ \text{14c} \\ \text{14d} \\ \text{14e} \\ \text{14f} \end{matrix}$$

The species' activities are computed by solving locally a set of 9 equations (one for each reaction) and 9 unknown (one for each species). At the equilibrium we then have:

$$\boldsymbol{U} \cdot \boldsymbol{\alpha} - \boldsymbol{\Gamma} = 0 \quad (16)$$

$$\boldsymbol{S_e} \cdot \log \boldsymbol{\alpha} - \log \boldsymbol{K} = 0 \quad (17)$$

The system of N_s equations and N_s unknown is solved at each point of the domain through a global ODEs and DAEs node. The first N_s-N_r equations given by Eq. 16 incorporate the reaction kinetics and advection-diffusion processes while the following N_r equations provided by Eq. 17 are solved to simulate the equilibrium reactions. This solution process allows linking the equilibrium reactions to the transport equations without computing directly $\boldsymbol{r_e}$.

3. Results and Discussion

The operation of a SCW is simulated with the aim to observe the THG behavior of the system and to study the influence of the bleed on the temperature, the concentration of Ca^{2+} and the reaction rate of calcite. This example considers the heating and cooling loads presented in Figure 3 and a total pumping rate $\dot{V}$ of 0.003 m^3/s. The simulated year starts on January 1 for a duration of 365 days. The initial water concentration is at the chemical equilibrium and is defined using equilibrium constants. The initial pH is 7 while the partial pressure of CO_2 is set to 4.1e-2 atm.

To analyze the influence of the bleed on the species' activity, two simulations have been done. The first simulation has been done with *B=0*, meaning that all the pumped water is re-injected at the top of the well while the second one has been done with *B=0*.15, meaning that 15% of the water is discharged in an injection well. Notice that in this work the injection is not simulated.

Figures 4a) and 4b) show the temporal evolution of the temperature and concentration of Ca^{2+} at the inlet and outlet of the well, for *B=0* and *B=0.15*. The results show that the temperature and the concentration of Ca^{2+} follow an opposite trend. In winter, when the temperature in the well is low, the concentration of Ca^{2+} is high. In contrast, the opposite behavior is observed in summer. This behavior may indicate that dissolved Ca^{2+} is likely to precipitate in the system's components in summer and thus, decrease the concentration of Ca^{2+} in the groundwater circulating in the well and surrounding aquifer.

To simplify the analysis of the rates of reaction of Eq. 8a) to 8c), the overall rate of precipitation and dissolution of calcite is used. The latter is given by the following equation (Plummer *et al.*, 1978):

$$R = k_1 \cdot \alpha_1 + k_2 \cdot \alpha_5 + k_3 \cdot \alpha_{H_2O} - k_{-1} \cdot \alpha_3 \cdot \alpha_2 - k_{-2} \cdot \alpha_3 \cdot \alpha_2^2 - k_{-3} \cdot \alpha_3 \cdot \alpha_2 \cdot \alpha_4 \quad (18)$$

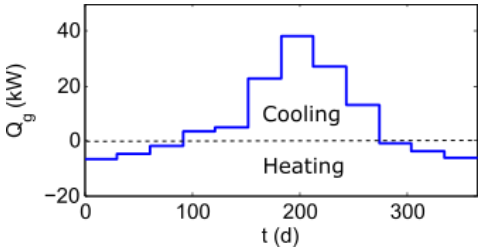

Figure 3. Illustration of the heating and cooling loads used in the simulations.

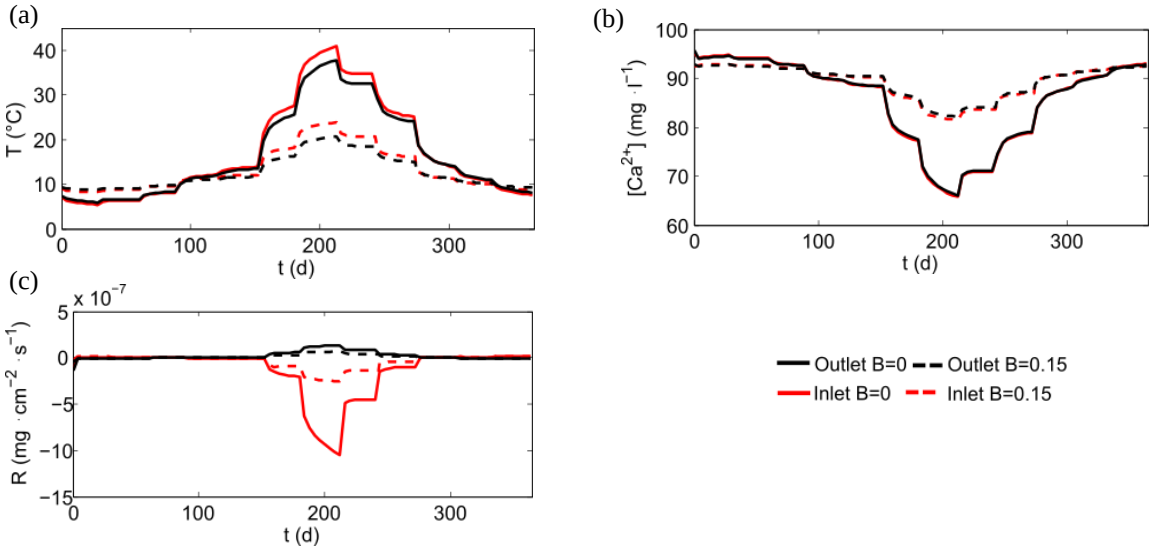

Figure 4. Temporal evolution of (a) the temperature, (b) the concentration of Ca^{2+} and (c) the reaction rate of calcite at the inlet and outlet of the well.

A positive value of R indicates that the direct reaction rate is higher than the reverse reaction rate, indicating dissolution of calcite. Negative *R* value indicates the opposite process, corresponding to precipitation in the system. Figure 4 c) presents the overall reaction rate of calcite *R* as a function of time. The results show that precipitation of calcite is likely to appear in summer at the inlet of the well within the descending fluid while calcite dissolution may take place within the riser pipe. The same behavior is presented in Figure 5 after 200 days of simulation. The occurrence of both processes in the same well but at different places is explained by the fact that when precipitation appears, the concentration of Ca^{2+} in solution decreases, leading to a state of undersaturation when temperature decreases.

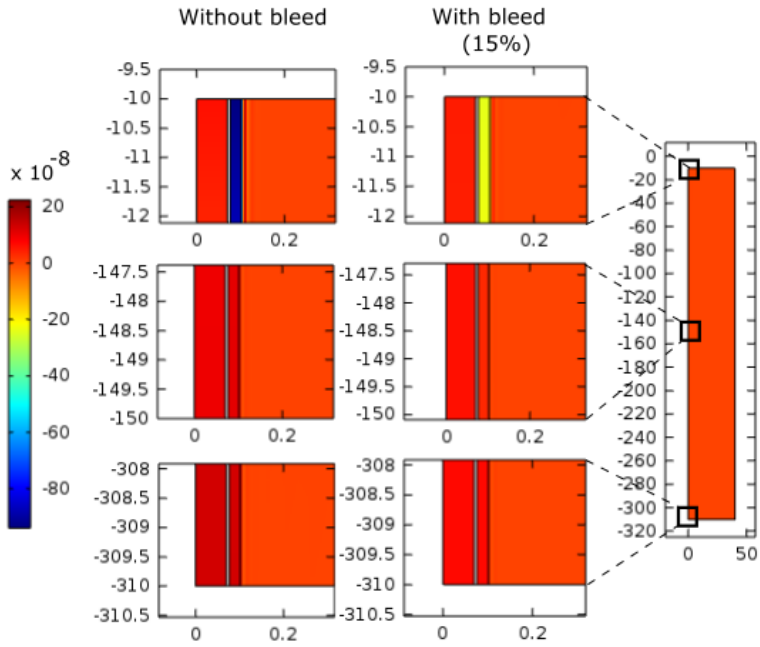

Figure 5. Spatial variation of the reaction rate of calcite (mg/(cm^2·s)) in the system, without bleed and with a 15% bleed at t=200 days.

Based on these results, one can therefore assume that in a SCW during summer, calcite is likely to precipitate at the inlet of the well. The solid particles may then possibly fall and accumulate in the pumping chamber, but also in the piping and mechanical equipments where heat exchange occurs.

Finally, the results show that the bleed has an important influence on the temperature and precipitation. With a certain amount of water discharged, the variation of temperature and concentration of Ca^{2+} are less. Moreover, the reaction rate of calcite is also more stable and the system is closer to the chemical equilibrium than without bleed. Thereby, the potential of precipitation and dissolution in the system is decreased.

4. Conclusions

In this paper, a coupled THG model implemented in Comsol Multiphysics was presented. Using three different physics from the Subsurface flow module (Darcy's Law, Heat transfer in porous media and Solute transport) and the ODEs and DEAs node, the presented model allows simulating the THG processes occurring in a SCW installed in a calcareous aquifer.

The results show that concentration of Ca^{2+} is highly dependent on the temperature and that both parameters have an inverse behavior. Calcite precipitation is highlighted by a decrease of Ca^{2+} in solution promoted in summer when the temperature within the well is high. Moreover, the results indicate that the reaction rate of calcite varies vertically in the well.

The influence of the bleed on the behavior of the system has been investigated. Our results indicate that the bleed tends to stabilize the temperature and activity of Ca^{2+} and thus to limit the risk of precipitation of calcite. This work is the first evidence that SCW bleed may be an important mitigation method against mineral precipitation and dissolution.

5. References

1. Abu-Nada, E., Akash, B., Al-Hinti, E., Al-Sarkhi, A., Nijmeh, S., Ibrahim, A., Modeling of a Geothermal Standing Column Well, *Int J Energy Res*, **32**, 306-317 (2008).
2. Deng, Z., Rees, S., Spitler, J., A Model for Annual Simulation of Standing Column Well Ground Heat Exchangers, *HVAC&R Research*, **11**, 637-655 (2005).
3. Holzbecher, E., *Environmental Modeling Using Matlab 2nd ed.*, 410 pages. Springer Berlin Heidelberg, Heidelberg, Germany (2012).
4. Lunardini, V, *Heat transfer in Cold Climates*, 731 pages. Van Nostrand Reinhold Co, Toronto, Canada (1981).
5. Morel, F.M.M., Hering, J.G., *Principles and Applications of Aquatic Chemistry*, 588 pages. Wiley-Interscience, Hoboken, United-States (1993).
6. Ng, B.M., Underwood, C.P., Walker, S.L., Standing Column Wells – Modeling the potential for Applications in Geothermal Heating and Cooling, *HVAC&R Res*, **6**, 1089-1100 (2011).
7. Nguyen, A., Pasquier, P., Marcotte, D., Multiphysics Modelling of Standing Column Well and Implementation of Heat Pumps Off-loading Sequence, in Comsol Conference, Boston, USA, (2012).
8. Nguyen, A., Pasquier, P., Marcotte, D., Thermal Resistance and Capacity Model For Standing Column Wells Operating Under a Bleed Control, *Renewable Energy*, **76**, 743-756 (2015).
9. Nguyen, A., Pasquier, P., Marcotte, D., Influence of Groundwater Flow in Fractured Aquifers on Standing Column Wells Performance, *Geothermics*, (2015) In Press.
10. Plummer, L.N., Wigley, T.M.L., Parkhurst, The Kinetics of Calcite Dissolution in CO_2-Water Systems at 5 to 60°C and 0 to 1 atm CO_2, *Am Jour Sci*, **278**, 179-216 (1978).
11. Rees, S.J., Spitler, J.D., Deng, Z., Orio, C.D., Johnson, C.N., A Study of Geothermal Heat Pump and Standing Column Well Performance, *ASHRAE Trans*, **110**, 3-13 (2004).
12. Saaltink, M.W., Ayora, C., Carrera, J., A Mathematical Formulation for Reactive Transport that Eliminates Mineral Concentrations, *Water Resources Research*, **33**, 1649-1656 (1998).